

1 Experimental test of microbiome protection across pathogen doses reveals importance of resident
2 microbiome composition

3

4 Running title: Variable pathogen protection by microbiomes

5

6 Chava L. Weitzman^{1*}

7 Bahman Rostama²

8 Courtney A. Thomason^{1,3}

9 Meghan May²

10 Lisa K. Belden¹

11 Dana M. Hawley¹

12

13 ¹ Department of Biological Sciences, Virginia Tech, Blacksburg, VA, USA

14 ² Department of Biomedical Sciences, University of New England, Biddeford, ME, USA

15 ³ Tennessee Department of Environment and Conservation, Division of Remediation, Oak Ridge,
16 TN, USA

17 * corresponding author: Department of Biological Sciences (MC 0406), Virginia Tech, 926 West
18 Campus Dr., Blacksburg, VA, 24060 USA; E-mail: clweitzman@vt.edu

19

20 **Keywords:** bird, conjunctivitis, *Mycoplasma gallisepticum*, house finch, ocular microbiome,
21 host–microbe interactions

22

23

24 **Summary**

25 Bacterial communities can be key in protecting hosts against pathogens, but that protection
26 depends on which bacteria make up resident communities during pathogen invasion.

27

28 **Abstract**

29 The commensal microbes inhabiting a host tissue can interact with invading pathogens and host
30 physiology in ways that alter pathogen growth and disease manifestation. Prior work in house
31 finches (*Haemorhous mexicanus*) found that resident ocular microbiomes were protective against
32 conjunctival infection and disease caused by a relatively high dose of *Mycoplasma gallisepticum*
33 (MG). Here, we used wild-caught house finches to experimentally examine whether protective
34 effects of the resident ocular microbiome vary with the dose of invading pathogen. We
35 hypothesized that commensal protection would be strongest at low MG inoculation doses
36 because the resident microbiome would be less disrupted by invading pathogen. Our five MG
37 dose treatments were fully factorial with an antibiotic treatment to perturb resident microbes just
38 prior to MG inoculation. Unexpectedly, we found no indication of protective effects of the
39 resident microbiome at any pathogen inoculation dose, which was inconsistent with prior work.
40 The ocular bacterial communities at the beginning of our experiment differed significantly from
41 those previously reported in local wild-caught house finches, likely causing this discrepancy.
42 These variable results underscore that microbiome-based protection in natural systems can be
43 context dependent, and natural variation in community composition may alter the function of
44 resident microbiomes in free-living animals.

45

46 **Introduction**

47 Understanding the varied roles of microbial communities in mediating host-pathogen
48 interactions across ecological contexts has become increasingly important. Bacterial community
49 members can interact with invading pathogens along the spectrum from facilitative to
50 antagonistic interactions (Daskin and Alford 2012; Boon *et al.* 2014; Oliver, Smith and Russell
51 2014; Becker *et al.* 2015b). Evidence of antagonistic interactions, whereby bacterial taxa inhibit
52 pathogens in or on a host, has been found across multiple host-pathogen systems. In some cases,
53 the structure of the microbial community at the site of pathogen invasion is predictive of disease
54 severity (Lauer *et al.* 2008; Becker *et al.* 2015a; Holden *et al.* 2015; Harris, Roode and Gerardo
55 2019). Further, studies using antibiotics to perturb resident microbiomes have found increases in
56 host morbidity and mortality when challenged with a pathogen, including higher pathogen loads
57 and greater sickness behaviors (Sekirov *et al.* 2008; Becker and Harris 2010; Weyrich *et al.*
58 2014; Holden *et al.* 2015; Kugadas *et al.* 2016; Thomason *et al.* 2017b). These results indicate
59 that intact microbiomes, i.e. resident microbiomes unmanipulated by antibiotics, often act in a
60 protective role for hosts.

61 Indeed, microbiomes play an important part in a host's innate immune system. Where
62 they interact directly with invading pathogens, microbial communities may act as the first line of
63 defense against invasion. Bacterial communities can inhibit invading pathogens through direct
64 and indirect interactions (Sassone-Corsi and Raffatellu 2015; McLaren and Callahan 2020). For
65 example, some cutaneous bacteria produce metabolites that inhibit growth of an invading fungal
66 pathogen on frogs and salamanders (Brucker *et al.* 2008a, 2008b; Becker *et al.* 2009; Harris *et al.*
67 2009). In other instances, commensal bacteria may outcompete pathogens for space or nutrients
68 (Sassone-Corsi and Raffatellu 2015; Wei *et al.* 2015; McLaren and Callahan 2020). Microbes
69 also help to maintain and trigger immune responses against pathogen invasion and disease, both

70 locally and elsewhere in the body (Ichinohe *et al.* 2011; McDermott and Huffnagle 2014; Thaiss
71 *et al.* 2016; Shukla *et al.* 2017). When resident microbiomes are experimentally disrupted,
72 pathogens can even exhibit distinct virulence phenotypes (Thomason *et al.* 2017b). Thus,
73 microbes can inhibit infection and disease severity in hosts via a range of potential mechanisms.

74 Overall, intact microbiomes appear to provide protection from infection and disease
75 across a variety of hosts and pathogens, but the extent of protection that the microbiome provides
76 is likely to depend on the dose of invading pathogen. Pathogen exposure dose predicts the degree
77 of resulting host morbidity and mortality in diverse disease systems (e.g. Ebert, Zschokke-
78 Rohringer and Carius 2000; Brunner, Richards and Collins 2005; Leon and Hawley 2017);
79 however, potential interactions between the host microbiome and pathogen dose on infection
80 outcomes have rarely been examined. In one study, the presence of an intact microbiome
81 increased the infective dose of *Bordetella pertussis* in mice by three orders of magnitude
82 compared with infective doses in mice given antibiotics to knock down the native microbiome
83 (Weyrich *et al.* 2014), consistent with the hypothesis that microbiome-mediated protection may
84 vary with pathogen dose. In natural systems, pathogen exposures commonly occur at low doses,
85 which may not, in single exposure events, cause disease (Dhondt *et al.* 2007; Regoes 2012;
86 Aiello *et al.* 2016). Heterogeneity of disease and pathogen load in animal populations could
87 result, in part, from the interplay between exposure dose and host protection by the microbiome.

88 In this study, we experimentally assessed the hypothesis that the degree of protection
89 provided by intact microbiomes varies with the dose of invading pathogen. House finches
90 (*Haemorhous mexicanus*) develop mycoplasmal conjunctivitis after infection by the bacterial
91 pathogen *Mycoplasma gallisepticum* (MG) (Kollias *et al.* 2004). Previous experimental work in
92 this system using ocular antibiotics found protective effects of the ocular microbiome against

93 MG conjunctival infection loads and disease severity (Thomason *et al.* 2017b). Treatment with
94 antibiotics prior to inoculation was also associated with increased activity of known virulence-
95 associated phenotypes (sialidase activity and cytadherence) in output MG isolates. Thus, while
96 the exact causal mechanisms remain unclear, intact ocular microbiomes appear to provide
97 protection against both MG infection and disease when inoculation doses are relatively high, as
98 was the case in Thomason *et al.* (2017b). MG also interacts with the resident microbiome to
99 cause shifts in the ocular bacterial community composition after MG invasion (Thomason *et al.*
100 2017a).

101 To assess potential interactions between pathogen invasion dose and the resident ocular
102 microbiome, here we compared infection and disease severity in control and antibiotic-perturbed
103 microbiome treatments for each of five MG inoculation dose concentrations. We perturbed the
104 ocular microbiome with cefazolin, a β -lactam antibiotic to which MG is intrinsically resistant
105 due to absence of a cell wall. After microbiome treatment (antibiotics or control), birds were
106 conjunctivally inoculated with a given MG dose. We monitored pathology and MG loads in the
107 conjunctiva throughout infection, and measured sialidase activity in output MG isolates at peak
108 infection. We predicted that the protective effects of intact ocular microbiomes would be
109 strongest at lower infective pathogen doses, because the microbiome would be less disrupted by
110 invading pathogen.

111

112 **Methods**

113 *Bird capture*

114 Hatch-year house finches ($n = 107$) were captured from June–August 2019 in
115 Montgomery County, Giles County, and Radford, Virginia. Birds were housed singly or in pairs

116 in cages (76 x 46 x 46 cm) and were provided a constant 12:12 photoperiod and food and water
117 *ad libitum*. We monitored birds for signs of disease every 3–5 days post-capture for two weeks
118 and then collected blood samples to assess MG-specific antibody concentrations. The
119 combination of age (hatch-year) and serological status allowed us to ensure that birds included in
120 our MG inoculation treatments did not have prior exposure to MG in the wild. No experimental
121 birds had conjunctivitis pathology at any point prior to inoculation, and only birds negative for
122 anti-MG antibodies (Hawley *et al.* 2011) were included in treatment groups inoculated with MG
123 (see *Experimental Design*). Birds were single-housed starting 13 days before experimental MG
124 inoculation (i.e. post-inoculation day (“PID”) -13). Birds were captured under VDGIF (061440)
125 and USFWS (MB158404-0) permits. Experimental procedures were approved by Virginia
126 Tech’s Institutional Animal Care and Use Committee.

127

128 *Experimental Design*

129 Experimental birds were divided among ten treatment groups in a fully factorial design
130 (Table 1), with the highest MG concentration similar to that used by Thomason *et al.* (2017b).
131 Treatment groups had as close to 50:50 sex ratios as possible. For logistical purposes, birds were
132 split between two temporal groups, with all treatments present in each group and a four-week lag
133 between the first and second group. Because birds given the lowest dose in the first temporal
134 group did not develop any pathology, we reallocated birds in the second temporal group to focus
135 on higher dose treatments.

136 We used ocular administration of the β -lactam antibiotic cefazolin to disrupt the resident
137 microbiome, as previously described (Thomason *et al.* 2017b). Cefazolin was rehydrated in PBS
138 and diluted to 33 mg/mL in artificial tears (Bausch + Lomb Advanced Eye Relief Dry Eye). We

139 administered the antibiotic by droplet instillation of 15 μ L into each conjunctiva three times per
140 day (8:00, 12:30, 17:00) for five days (Figure 1). Because saline administration as a control may
141 have disrupted the resident microbiome, control catch-only birds were caught at the same times
142 as those given the antibiotic, held briefly, and released. We used culture techniques to confirm
143 the effectiveness of the antibiotic in reducing resident conjunctival bacterial populations
144 (Supplemental Materials).

145 We inoculated house finches with the VA1994 MG isolate (7994-1 6 P 9/17/2018)
146 because the ocular microbiome provided protection against this isolate in prior work (Thomason
147 *et al.* 2017b). MG was diluted in antibiotic-free Frey's broth medium on the day of inoculation.
148 Experimental birds were inoculated by droplet instillation with 70 μ L of MG diluted to a given
149 concentration (depending on their dose treatment), split between the two conjunctiva (i.e.
150 approximately 35 μ L per eye). Infection controls ("MG controls", Table 1) were given 70 μ L of
151 antibiotic-free Frey's media.

152

153 *Pathology, Swabbing, and MG Quantification*

154 We collected pathology data and conjunctival swab samples from birds at multiple
155 timepoints from PID -13 to PID 27 (Figure 1). Pathology was scored for each conjunctiva on a
156 0–3 scale, with scores made while blind to a given bird's treatment. Briefly, no clinical signs of
157 conjunctivitis is scored as 0, a score of 1 represents minor swelling around the eye or minor
158 conjunctival eversion, moderate swelling and eversion is scored as 2, and severe swelling,
159 eversion, and exudate is scored as 3 (Sydenstricker *et al.* 2005). We summed the scores between
160 the two sides within each time point, resulting in a value from 0–6 per bird per time point
161 (Hawley *et al.* 2011). No experimental birds had signs of disease before inoculation. After

162 measuring pathology, we swabbed the conjunctiva with flocked swabs (Copan FLOQSwabs,
163 Copan Diagnostics Inc., Murrieta, CA) lubricated with artificial tears, combining the two swabs
164 from each bird into 300 μ L Zymo DNA/RNA Shield (Zymo Research, Irvine, CA). On PID -1, a
165 subset of birds' conjunctival swabs were cultured to confirm the antibiotic effectiveness
166 (Supplemental Materials). On PID 8, after the DNA/RNA-preserved swab, we swabbed the
167 conjunctivae a second time for MG culture and phenotyping of sialidase activity. On the day of
168 collection, MG phenotype swabs from MG treatment groups were shipped on ice to the
169 University of New England in 3.0 mL Remel M5 media, where they were subjected to a sialidase
170 activity assay after growth as previously described (Thomason *et al.* 2017b) (Supplemental
171 Materials).

172 DNA was extracted from conjunctival swab samples from PID -1, 3, and 13 with the
173 Qiagen DNeasy Blood and Tissue kit (Qiagen, Valencia, CA) protocol for Gram-positive
174 bacteria (see Supplemental Materials for modifications). To quantify MG in swab samples, we
175 conducted quantitative PCR (qPCR) on the MGC2 gene as previously described (Hawley *et al.*
176 2013), with pathogen load analyzed as $\log_{10}(\text{load}+1)$. Data from PID -1 was used to verify that
177 the birds did not have MG prior to experimental inoculation.

178

179 *Statistical Analyses*

180 We used R v4.0.2 in RStudio v1.3.1093 to conduct all statistical analyses (R
181 Development Core Team 2015; RStudio Team 2020). First, we tested the effectiveness of the
182 antibiotic in knocking down the resident ocular microbiomes, comparing optical density (OD)
183 values of cultured swab samples between antibiotic and catch-only (microbiome control) birds
184 using ANOVA. We then analyzed pathology, pathogen load, probability of infection (defined

185 below), and MG sialidase phenotype data to detect how the interaction between microbiome
186 treatment and MG dose affected infection and disease severity. We used these analyses
187 specifically to test the prediction that ocular microbiomes have stronger protective effects at
188 lower pathogen infective doses. We ran analyses on data from all experimental birds, as well as a
189 dataset including only birds inoculated with MG. These two datasets provided similar results, so
190 below we present analyses of just MG-inoculated birds (see Supplemental Materials for full data
191 set results).

192 To determine the effects of MG dose and microbiome treatments on disease severity over
193 time, we modelled pathology data after inoculation using negative binomial generalized linear
194 mixed effects models (GLMM) in the glmmTMB package (Brooks *et al.* 2017), with bird ID as a
195 random variable. We used model simplification to arrive at a minimal model addressing our
196 question, sequentially removing interaction terms and covariates with $p < 0.1$ from Wald's chi-
197 squared tests using the car package (Fox and Weisberg 2019). The full model included
198 interactions between MG dose ($\log_{10}(\text{MG concentration} + 1)$) and PID, MG dose and
199 microbiome treatment, and microbiome treatment and PID, along with sex and temporal group as
200 covariates. Regardless of p-value, MG dose and microbiome treatment were kept in the final
201 model, though we removed their interaction from the model where applicable. We used Akaike
202 information criterion (AIC) to determine if a better model fit was provided if MG dose or PID
203 were analyzed as quadratic variables ($\log_{10}(\text{MG concentration} + 1)^2$ and PID^2 , respectively).

204 To determine if pathogen load (our metric of infection severity) differed among the
205 treatment groups, we analyzed load data from PID 3 and 13 using linear mixed effects models in
206 the lme4 package (Bates *et al.* 2015). We conducted model simplification as above, except PID
207 was only included as an ordinal variable because we had fewer time points available.

208 Pathogen load data were also used to assess successful infection in experimental birds,
209 conservatively defined as any post-inoculation MG load ($\log_{10}(\text{load} + 1)$) greater than $3.1 \log_{10}$
210 copies as per prior work (Adelman *et al.* 2015; Leon and Hawley 2017). We analyzed whether
211 microbiome treatment affected the probability of infection using binomial GLM with a probit
212 link. The main predictor variables of interest included the interaction between microbiome and
213 MG dose treatments, with host sex and temporal group as covariates.

214 When sialidase activity was present in the cultured MG isolates from PID 8, sialidase
215 activity (mU/mg total protein) was analyzed using ANOVA, with the same predictor variables as
216 in the probability of infection analyses.

217

218 *Describing Starting Ocular Microbiomes*

219 A subset of ocular swab samples were used to compare the resident ocular microbiomes
220 in birds at the beginning of this experiment with those in a previous study assessing the effect of
221 antibiotics on responses to MG (Thomason *et al.* 2017b). In order to describe the resident
222 microbial community without confounding effects of experimental perturbation, samples used
223 here were collected either prior to ocular antibiotic treatment at PID -13 (n = 7) or on PID -1
224 from catch-only birds (n = 4 microbiome controls). We used the Zymo Quick DNA/RNA
225 Microprep extraction kit (Zymo Research, Irvine, CA) to extract samples, eluting in 15 μL
226 DNase/RNase-free water. We conducted library prep for Illumina MiSeq sequencing as
227 previously described, amplifying a portion of the V4 region of 16S bacterial rRNA using 515F
228 and barcoded 806R primers (Caporaso *et al.* 2012; Thomason *et al.* 2017a). Single-end sequence
229 reads were demultiplexed using QIIME2, and reads were trimmed and quality-filtered with a
230 maximum of two expected errors using the DADA2 package (Callahan *et al.* 2016; Bolyen *et al.*

231 2019). We similarly filtered and trimmed reads from 14 microbiome control PID -1 samples
232 from Thomason *et al.* (2017b), and combined those reads from 2016 with our 2019 data set to
233 denoise reads to detect amplicon sequence variants (ASVs) with DADA2. Sample collection
234 protocols differed for the 2016 dataset (which used sterile cotton swabs, storage in tryptose
235 phosphate broth, and DNA extraction with Qiagen DNeasy Blood and Tissue Kit), but PCR and
236 sequencing protocols were identical; thus, the datasets should be broadly comparable (Fouhy *et*
237 *al.* 2016; Panek *et al.* 2018; Bjerre *et al.* 2019). We assigned taxonomy to our combined read file
238 with the Silva v132 database and filtered out non-bacterial, chloroplast, and mitochondrial reads.
239 Sequences are openly available on figshare (DOI: 10.6084/m9.figshare.14541390; temporary
240 link: <https://figshare.com/s/ce3aea67c701bb061b48>).

241 We used analysis of composition of microbiomes (ANCOM) on unrarefied data in
242 QIIME2 to assess differential abundance of bacterial genera between the two study years. After
243 inspecting rarefaction curves, we rarefied the data to 7,500 reads per sample, removing three
244 samples from the 2016 data. We used QIIME2 to calculate ASV richness, alpha diversity metrics
245 (Pielou's evenness, Shannon's diversity metric, and Faith's phylogenetic diversity) and beta
246 diversity (weighted and unweighted UniFrac distances). Analyses of these metrics focused on
247 detecting differences between the study years in starting microbial communities in absence of
248 antibiotic perturbation and prior to pathogen inoculation. We compared ASV richness and alpha
249 diversity metrics between the sampling years with Kruskal-Wallis tests. With the vegan package
250 (Oksanen *et al.* 2018), we compared beta diversities between sampling years with
251 PERMANOVA and further tested for differences in multivariate dispersion with permutational
252 multivariate analysis of beta-dispersion.

253

254 **Results**

255 Culture-based assays indicated that the topical ocular antibiotic significantly suppressed
256 the overall abundance of viable resident bacteria (Figure S1), consistent with prior work
257 (Thomason et al. 2017b) and indicating that our microbiome antibiotic treatment successfully
258 perturbed the resident ocular microbiome. Following antibiotic treatment, but just prior to MG
259 inoculation (PID -1), none of the experimental birds had pathology or detectable MG by qPCR.

260

261 *Disease Severity*

262 Overall, we found no support for our primary hypothesis that MG dose and microbiome
263 antibiotic treatment would interact to influence disease severity. Both MG dose and PID were
264 significant predictors of disease severity in our simplified model (Table 2), with pathology score
265 increasing with MG dose, consistent with prior work (Leon and Hawley 2017). However,
266 microbiome perturbation with antibiotics was not significantly predictive of disease severity
267 (Table 2), either alone or in interaction with MG dose, such that the interaction was removed
268 during model simplification. Antibiotic treated birds generally had lower pathology scores, in the
269 opposite direction of prior work (Thomason et al. 2017b), although this was not statistically
270 significant ($p = 0.055$; Figure 2a, Figure S2). Because a single house finch in the catch-only
271 (microbiome control), 3×10^3 CCU/mL MG dose treatment had abnormally high pathology scores
272 from PID 8 onward, we also evaluated the simplified model without this individual. This analysis
273 suggested that this one individual was important in driving the marginal effects of microbiome
274 treatment on pathology (Table 2).

275

276 *Pathogen Load and Probability of Infection*

277 We used linear mixed effects models to detect effects of microbiome treatment and MG
278 dose on infection loads quantified on post-inoculation days 3 and 13. Similar to the results for
279 disease severity, we found no support for interactions between MG dose and microbiome
280 treatment on infection load. In the simplified model, MG load was significantly predicted by MG
281 dose, PID, and their interaction, but not microbiome treatment (Table 2, Figure 2b).

282 We further used pathogen load to determine if the birds were successfully infected and
283 whether probability of infection differed with microbiome and MG dose treatments. Consistent
284 with MG load results, probability of infection differed based on MG dose, but not microbiome
285 antibiotic treatment, with birds given higher MG doses more likely to become infected (Table 2).

286

287 *MG Sialidase Phenotype*

288 Of the 85 birds inoculated with MG, 48 cultured swab samples from PID 8 grew and
289 exhibited sialidase activity (MG doses: 3×10^1 n = 1; 3×10^2 n = 4; 3×10^3 n = 20; 3×10^4 n = 23).
290 From linear models, only temporal group was a significant predictor of sialidase activity (Table
291 2, Figure S3), with MG isolated from birds in temporal group 2 exhibiting lower sialidase
292 activity. Neither microbiome treatment, nor MG dose, was significant.

293

294 *Resident Ocular Microbiomes*

295 Prior to MG inoculation, resident ocular microbiomes from the present experiment were
296 dominated by *Proteobacteria* and *Actinobacteria*, with *Sphingomonas*, *Pseudomonas*,
297 *Comamonas*, *Mycobacterium* and other genera in greater abundance in the 2019 samples based
298 on ANCOM compared with house finch conjunctival samples collected for a previous
299 experiment from birds captured and housed at the same localities and conditions (Thomason *et*

300 *al.* 2017b) (Figure 3, Table S4). In contrast, resident ocular microbiomes sampled in 2016 were
301 dominated by *Firmicutes*, with greater abundance of *Lactococcus* and *Enterococcus* in 2016
302 compared with our 2019 samples (Figure 3, Table S4). Though the genus *Lactococcus* was the
303 dominant taxon in finch ocular microbiomes in 2016, this genus accounted for less than 0.5% of
304 the reads in the three (of 11) 2019 samples where it was detected. All samples were collected
305 from ocular microbiomes that were not perturbed with antibiotics.

306 There were also quantifiable differences between study years with respect to alpha and
307 beta diversity of resident bacterial communities. Using Kruskal-Wallis tests, the 2016 and 2019
308 samples significantly differed in ASV richness and the three alpha diversity metrics ($p \leq 0.0001$
309 each; Table S2, Figure S4). Similarly, samples from the two study years significantly differed in
310 beta diversity (weighted and unweighted UniFrac $p = 0.001$; Table S3, Figure S5). Analysis of
311 dispersion detected significant differences in dispersion between the years ($p \leq 0.01$ each). Thus,
312 we found strong support for differences in microbiome composition and structure between
313 studies.

314

315 **Discussion**

316 This experiment assessed dose-dependent protective effects of the house finch ocular
317 microbiome against the conjunctival pathogen *Mycoplasma gallisepticum*. Although disease and
318 infection severity both increased with MG inoculation dose as expected based on previous work
319 in this and other systems (Timms *et al.* 2001; Regoes, Ebert and Bonhoeffer 2002; Spekreijse *et*
320 *al.* 2011; Leon and Hawley 2017), we did not detect the presence of protective effects of the
321 intact microbiome at any inoculation dose, including the dose used in prior work that found
322 significant protective effects of intact ocular microbiomes (Thomason *et al.* 2017b). Thus, we

323 were unable to adequately test whether protective effects of the ocular microbiome are dose-
324 dependent. Instead, we show that variation in the resident microbiome present in the conjunctiva
325 at the time of pathogen inoculation likely explains the discrepancies between ours and the
326 previous study. This and other studies finding that microbiome variation at the time of pathogen
327 invasion predict variation in disease (e.g. Becker *et al.* 2015a; Walke *et al.* 2015; Nava-González
328 *et al.* 2021) underscore the potential for microbiome function to be highly variable and context-
329 dependent in natural systems.

330 We found that the ocular microbiomes at the start of this experiment differed notably
331 from those in previous experiments (Thomason *et al.* 2017a, 2017b), such that the bacteria
332 contributing to the microbiome's protective effects in Thomason *et al.* (2017b) were likely not
333 present or were very rare in our study. Specifically, the ocular communities in birds in 2016,
334 where protective effects of the ocular microbiome were detected, were largely comprised of the
335 bacterial genus *Lactococcus*, with over 70% of the relative abundance representing this genus. A
336 high relative abundance of *Lactococcus* was also documented in another prior study describing
337 ocular bacterial microbiomes and their shifts after MG inoculation (Thomason *et al.* 2017a).
338 *Lactococcus* can inhibit growth of other bacteria through lactic acid production and other
339 antimicrobial metabolites, and lactic-acid-producing bacteria can provide important protection
340 when they dominate a microbiome (Røssland *et al.* 2005; Vásquez *et al.* 2012; O'Hanlon,
341 Moench and Cone 2013). In birds from the present experiment, which were captured from the
342 same areas of Virginia as finches in past studies, we found that *Lactococcus* comprised less than
343 1% of the ocular communities. Importantly, the two groups of microbiome samples were
344 collected and processed under slightly different protocols, which may explain some of the
345 variation between sampling years, given that microbiome studies often find differences in

346 community composition and diversity across extraction protocols (Fouhy *et al.* 2016; Bjerre *et*
347 *al.* 2019). However, distinct extraction protocols are unlikely to cause the degree of divergence
348 between predominant taxa detected between the two studies here (Figure 3). Overall, the low
349 abundance of *Lactococcus* and large shift in the resident microbiome compared to previous
350 descriptions could have resulted in its lack of protective function against mycoplasmal
351 conjunctivitis in this study. Further, the dominant ocular community members in this experiment
352 may not have responded to experimental antibiotic treatment in the same way as the prior
353 *Lactococcus*-dominated communities, potentially limiting our ability to adequately disrupt the
354 ocular microbial community and thus test its protective function. Though we used culture-based
355 methods to verify that administering cefazolin reduced ocular bacterial growth in this study, we
356 also detected abundant genera in the sequenced ocular samples that may not be susceptible to
357 this antibiotic, such as *Pseudomonas* and *Sphingomonas* (Reller *et al.* 1973; Mustafa, Maulud
358 and Hamad 2018). Thus, it is challenging to compare the role of these distinct ocular
359 communities in ocular health and disease.

360 Past work also found that perturbing the ocular microbiome increased activity of sialidase
361 enzymes associated with MG virulence (Thomason *et al.* 2017b), and that activity was correlated
362 with variation in disease severity among individuals. Here, we did not detect any influence of
363 ocular microbiome disruption on the sialidase activity of output MG isolates, consistent with the
364 absence of significant effects of antibiotics on disease severity. Modulation of sialidase activity,
365 and often its functional balance with host cell cytadherence, are important mechanisms for fine-
366 scale rheostasis (i.e. regulation in a changing environment) during infection for many pathogens.
367 Overall, the differences between these results and those of past work suggest that prior protective
368 effects, including the potential modulation of sialidase activity in MG, were likely driven by

369 *Lactococcus* and other resident community members that were largely absent in the resident
370 ocular microbiomes in this experiment.

371 The limited data on avian ocular microbiomes restricts our ability to discern the
372 microbiome composition that should be considered “normal” or expected in house finches.
373 Though no other studies beyond those discussed above have described ocular communities in
374 birds with high throughput sequencing, samples from non-human mammals have found
375 *Proteobacteria*, *Actinobacteria*, and *Firmicutes* on ocular surfaces, with the predominant phylum
376 differing among and within host species (Alfano *et al.* 2015; Leis and Costa 2019; Leis, Madruga
377 and Costa 2021). The abundant genera within those mammals, however, do not overlap with the
378 principal genera in house finches. As with other microbiomes with such high exposure to the
379 environment (e.g. skin, respiratory tract), the bacteria in ocular samples are likely affected by
380 transient taxa that are detected in the eye, but are not true commensals (Lauer *et al.* 2007; Kong
381 and Segre 2012; Hammer, Sanders and Fierer 2019). Further, the house finch ocular
382 microbiomes that have been described have all derived from captive birds, and studies from
383 other systems show that captivity can strongly affect microbiomes (e.g. Cheng *et al.* 2015; Kohl
384 *et al.* 2017). The birds in this experiment and in the first study characterizing house finch ocular
385 microbiomes (Thomason *et al.* 2017a), which found *Lactococcus* predominating in the
386 microbiome, were housed in captivity for approximately two to four months prior to MG
387 inoculation. Thus, time in captivity is unlikely to explain the large differences in abundance of
388 *Lactococcus* between studies. The two studies directly compared here (Figure 3) both included
389 hatch-year males and females captured from the same population in SW Virginia during summer
390 and housed under identical captive conditions in the same laboratory space, though other
391 unrecognized differences in housing and care among the years could have affected the ocular

392 communities at the beginning of the experiments. Overall, the microbial differences between
393 study years represent, at least in some capacity, differences across years between the
394 microbiomes at the time of capture. Further study should quantify temporal variation in the
395 ocular microbiome of free-living house finches, as well as effects of captivity on such variation,
396 to begin to unravel the mechanisms that determine ocular microbial composition in house finches
397 and potentially other songbird taxa.

398 Large differences in microbial communities within a host species are common (e.g. Tung
399 *et al.* 2015; Escallón *et al.* 2017; Springer *et al.* 2017; Kueneman *et al.* 2019; Hernandez *et al.*
400 2020) and likely play a large role in the variation of other aspects of host ecology. Much of what
401 we know about patterns of microbiomes in and on wild organisms, particularly outside of the
402 gut, and their interactions with pathogens comes from research on amphibian skin microbiomes,
403 which can vary significantly with respect to spatial, temporal, and environmental factors (Walke
404 and Belden 2016; Familiar López *et al.* 2017; Christian *et al.* 2018; Kueneman *et al.* 2019;
405 Loudon *et al.* 2020; Douglas, Hug and Katzenbach 2021). Although studies of amphibian skin
406 microbiomes focus on interactions with invading fungal and viral pathogens, studies in other
407 natural systems are increasingly focusing on bacterial microbiome patterns and their functional
408 roles in and on wild animals (e.g. Kohl 2012; Ainsworth *et al.* 2015; Colston and Jackson 2016;
409 Thomason *et al.* 2017a; Allender *et al.* 2018; Weitzman, Sandmeier and Tracy 2018). While
410 most studies seek patterns among individuals, microbial communities are labile even within
411 single hosts, with microbial community shifts affected by factors such as horizontal transmission
412 from social interactions, season and food availability (particularly for the gut microbiome), and
413 infection (Jani and Briggs 2014; Bradley *et al.* 2016; Springer *et al.* 2017; Thomason *et al.*
414 2017a; Zhu *et al.* 2020). Much like the skin, ocular surfaces are constantly exposed to the outside

415 world. In humans, ocular microbiomes not only vary among individuals (Ozkan *et al.* 2018;
416 Delbeke *et al.* 2021), but also fluctuate across time within healthy individuals (Ozkan *et al.*
417 2017). Considering the many factors that could lead to temporal changes in microbial
418 communities, it is reasonable to expect that house finch ocular microbiomes differ among
419 generations and years. In this and other systems, changes in community composition across time
420 could affect the microbiome's protective role, because members of the community influence the
421 microbiome's effectiveness as protective. Thus, understanding the factors that drive changes in
422 microbial community composition and function in this and other natural systems is critical.

423 This experiment attempted to conceptually expand upon results generated four years ago,
424 by asking whether microbiome-mediated protection is dose dependent. Instead, we found that
425 intact microbiomes that provided significant protection from infection and disease in an earlier
426 experiment provided no detectable protection here, despite use of the same pathogen and free-
427 living host. While this lack of protection meant that we were unable to adequately test our
428 motivating hypothesis with respect to dose, the broader pattern of variable microbiome-mediated
429 protection against infection is likely a common occurrence in ecological studies, as many abiotic
430 and biotic changes occur across spatial and temporal scales that could affect ecological patterns.
431 The publication bias in ecological literature implies that many fields may be lacking the true
432 range of results needed to fully assess ecological hypotheses and their generalizability (Jennions
433 and Møller 2002; Fidler *et al.* 2017). Importantly, our study contributes to our understanding of
434 how and when the host microbiome is protective, and the context-dependency of interactions
435 between complex microbial communities and invading pathogens. With these considerations,
436 investigations should examine microbial variation, and associated potential inconsistencies of
437 results, when exploring functions of resident microbiomes in free-living animals.

438

439 **Funding**

440 This work was supported by the National Science Foundation [IOS-1755051, IOS-1755297].

441

442 **Acknowledgements**

443 Thank you to Sara Teemer, Marissa Langager, Allison Rowley, the rest of the Hawley lab, and

444 Emma Bradford for their help in the field and lab.

445

446 **Conflicts of interest**

447 The authors declare no conflicts of interest.

448

449 **References**

450 Adelman JS, Moyers SC, Farine DR *et al.* Feeder use predicts both acquisition and transmission
451 of a contagious pathogen in a North American songbird. *Proc Royal Soc B: Biological
452 Sci* 2015;282:20151429.

453 Aiello CM, Nussear KE, Esque TC *et al.* Host contact and shedding patterns clarify variation in
454 pathogen exposure and transmission in threatened tortoise *Gopherus agassizii*:
455 implications for disease modelling and management. *J Anim Ecol* 2016;85:829–42.

456 Ainsworth TD, Krause L, Bridge T *et al.* The coral core microbiome identifies rare bacterial taxa
457 as ubiquitous endosymbionts. *ISME J* 2015;9:2261–74.

458 Alfano N, Courtiol A, Vielgrader H *et al.* Variation in koala microbiomes within and between
459 individuals: effect of body region and captivity status. *Sci Rep* 2015;5:1–12.

460 Allender MC, Baker S, Britton M *et al.* Snake fungal disease alters skin bacterial and fungal
461 diversity in an endangered rattlesnake. *Sci Rep* 2018;8:12147.

462 Bates D, Mächler M, Bolker B *et al.* Fitting linear mixed-effects models using lme4. *J Stat Softw*
463 2015;67:1–48.

464 Becker MH, Brucker RM, Schwantes CR *et al.* The bacterially produced metabolite violacein is
465 associated with survival of amphibians infected with a lethal fungus. *Appl Environ
466 Microbiol* 2009;75:6635–8.

467 Becker MH, Harris RN. Cutaneous bacteria of the redback salamander prevent morbidity
468 associated with a lethal disease. *PLoS ONE* 2010;5:e10957.

469 Becker MH, Walke JB, Cikanek S *et al.* Composition of symbiotic bacteria predicts survival in
470 Panamanian golden frogs infected with a lethal fungus. *Proc Royal Soc B: Biological Sci*
471 2015a;282:20142881.

472 Becker MH, Walke JB, Murrill L *et al.* Phylogenetic distribution of symbiotic bacteria from
473 Panamanian amphibians that inhibit growth of the lethal fungal pathogen
474 *Batrachochytrium dendrobatidis*. *Mol Ecol* 2015b;24:1628–41.

475 Bjerre RD, Hugerth LW, Boulund F *et al.* Effects of sampling strategy and DNA extraction on
476 human skin microbiome investigations. *Sci Rep* 2019;9:17287.

477 Bolyen E, Rideout JR, Dillon MR *et al.* Reproducible, interactive, scalable and extensible
478 microbiome data science using QIIME 2. *Nat Biotechnol* 2019;37:852–7.

479 Boon E, Meehan CJ, Whidden C *et al.* Interactions in the microbiome: communities of
480 organisms and communities of genes. *FEMS Microbiol Rev* 2014;38:90–118.

481 Bradley CW, Morris DO, Rankin SC *et al.* Longitudinal evaluation of the skin microbiome and
482 association with microenvironment and treatment in canine atopic dermatitis. *J Invest*
483 *Dermatol* 2016;136:1182–90.

484 Brooks ME, Kristensen K, van Benthem KJ *et al.* glmmTMB balances speed and flexibility
485 among packages for zero-inflated generalized linear mixed modeling. *The R Journal*
486 2017;9:378–400.

487 Brucker RM, Baylor CM, Walters RL *et al.* The identification of 2,4-diacetylphloroglucinol as
488 an antifungal metabolite produced by cutaneous bacteria of the salamander *Plethodon*
489 *cinereus*. *J Chem Ecol* 2008a;34:39–43.

490 Brucker RM, Harris RN, Schwantes CR *et al.* Amphibian chemical defense: Antifungal
491 metabolites of the microsymbiont *Janthinobacterium lividum* on the salamander
492 *Plethodon cinereus*. *J Chem Ecol* 2008b;34:1422–9.

493 Brunner JL, Richards K, Collins JP. Dose and host characteristics influence virulence of
494 ranavirus infections. *Oecologia* 2005;144:399–406.

495 Callahan BJ, McMurdie PJ, Rosen MJ *et al.* DADA2: High-resolution sample inference from
496 Illumina amplicon data. *Nat Methods* 2016;13:581–3.

497 Caporaso JG, Lauber CL, Walters WA *et al.* Ultra-high-throughput microbial community
498 analysis on the Illumina HiSeq and MiSeq platforms. *ISME J* 2012;6:1621–4.

499 Cheng Y, Fox S, Pemberton D *et al.* The Tasmanian devil microbiome—implications for
500 conservation and management. *Microbiome* 2015;3:76.

501 Christian K, Weitzman C, Rose A *et al.* Ecological patterns in the skin microbiota of frogs from
502 tropical Australia. *Ecol Evol* 2018;8:10510–9.

503 Colston TJ, Jackson CR. Microbiome evolution along divergent branches of the vertebrate tree
504 of life: what is known and unknown. *Mol Ecol* 2016;25:3776–800.

505 Daskin JH, Alford RA. Context-dependent symbioses and their potential roles in wildlife
506 diseases. *Proc Royal Soc B: Biological Sci* 2012;279:1457–65.

507 Delbeke H, Younas S, Casteels I *et al.* Current knowledge on the human eye microbiome: a
508 systematic review of available amplicon and metagenomic sequencing data. *Acta*
509 *Ophthalmol* 2021;99:16–25.

510 Dhondt AA, Dhondt KV, Hawley DM *et al.* Experimental evidence for transmission of
511 *Mycoplasma gallisepticum* in house finches by fomites. *Avian Pathol* 2007;36:205–8.

512 Douglas AJ, Hug LA, Katzenback BA. Composition of the North American wood frog (*Rana*
513 *sylvatica*) bacterial skin microbiome and seasonal variation in community structure.
514 *Microb Ecol* 2021;81:78–92.

515 Ebert D, Zschokke-Rohringer CD, Carius HJ. Dose effects and density-dependent regulation of
516 two microparasites of *Daphnia magna*. *Oecologia* 2000;122:200–9.

517 Escallón C, Becker MH, Walke JB *et al.* Testosterone levels are positively correlated with
518 cloacal bacterial diversity and the relative abundance of Chlamydiae in breeding male
519 rufous-collared sparrows. *Funct Ecol* 2017;31:192–203.

520 Familiar López M, Rebollar EA, Harris RN *et al.* Temporal variation of the skin bacterial
521 community and *Batrachochytrium dendrobatidis* infection in the terrestrial cryptic frog
522 *Philoria loveridgei*. *Front Microbiol* 2017;8:2535.

523 Fidler F, Chee YE, Wintle BC *et al.* Metaresearch for evaluating reproducibility in ecology and
524 evolution. *BioScience* 2017;67:282–9.

525 Fouhy F, Clooney AG, Stanton C *et al.* 16S rRNA gene sequencing of mock microbial
526 populations- impact of DNA extraction method, primer choice and sequencing platform.
527 *BMC Microbiol* 2016;16:123.

528 Fox J, Weisberg S. *An R Companion to Applied Regression, Third Edition*. Thousand Oaks CA:
529 Sage., 2019.

530 Hammer TJ, Sanders JG, Fierer N. Not all animals need a microbiome. *FEMS Microbiol Lett*
531 2019;366:fnz117.

532 Harris EV, de Roode JC, Gerardo NM. Diet–microbiome–disease: Investigating diet’s influence
533 on infectious disease resistance through alteration of the gut microbiome. *PLoS Pathog*
534 2019;15:e1007891.

535 Harris RN, Brucker RM, Walke JB *et al.* Skin microbes on frogs prevent morbidity and mortality
536 caused by a lethal skin fungus. *ISME J* 2009;3:818–24.

537 Hawley DM, Grodio J, Jr SF *et al.* Experimental infection of domestic canaries (*Serinus canaria*
538 *domestica*) with *Mycoplasma gallisepticum*: a new model system for a wildlife disease.
539 *Avian Pathol* 2011;40:321–7.

540 Hawley DM, Osnas EE, Dobson AP *et al.* Parallel patterns of increased virulence in a recently
541 emerged wildlife pathogen. *PLoS Biol* 2013;11:e1001570.

542 Hernandez J, Escallón C, Medina D *et al.* Cloacal bacterial communities of tree swallows
543 (*Tachycineta bicolor*): Similarity within a population, but not between pair-bonded social
544 partners. *PLoS ONE* 2020;15:e0228982.

545 Holden WM, Hanlon SM, Woodhams DC *et al.* Skin bacteria provide early protection for newly
546 metamorphosed southern leopard frogs (*Rana sphenocephala*) against the frog-killing
547 fungus, *Batrachochytrium dendrobatidis*. *Biol Conserv* 2015;187:91–102.

548 Ichinohe T, Pang IK, Kumamoto Y *et al.* Microbiota regulates immune defense against
549 respiratory tract influenza A virus infection. *Proc Nat Acad Sci USA* 2011;108:5354–9.

550 Jani AJ, Briggs CJ. The pathogen *Batrachochytrium dendrobatidis* disturbs the frog skin
551 microbiome during a natural epidemic and experimental infection. *Proc Nat Acad Sci
552 USA* 2014;111:E5049–58.

553 Jennions MD, Møller AP. Publication bias in ecology and evolution: an empirical assessment
554 using the ‘trim and fill’ method. *Biol Rev* 2002;77:211–22.

555 Kohl K. Diversity and function of the avian gut microbiota. *J Comp Physiol B* 2012;182:591–
556 602.

557 Kohl KD, Brun A, Magallanes M *et al.* Gut microbial ecology of lizards: insights into diversity
558 in the wild, effects of captivity, variation across gut regions and transmission. *Mol Ecol*
559 2017;26:1175–89.

560 Kollias GV, Sydenstricker KV, Kollias HW *et al.* Experimental infection of house finches with
561 *Mycoplasma gallisepticum*. *J Wildlife Dis* 2004;40:79–86.

562 Kong HH, Segre JA. Skin Microbiome: Looking Back to Move Forward. *J Invest Dermatol*
563 2012;132:933–9.

564 Kueneman JG, Bletz MC, McKenzie VJ *et al.* Community richness of amphibian skin bacteria
565 correlates with bioclimate at the global scale. *Nature Ecol Evol* 2019;3:381–9.

566 Kugadas A, Christiansen SH, Sankaranarayanan S *et al.* Impact of microbiota on resistance to
567 ocular *Pseudomonas aeruginosa*-induced keratitis. *PLoS Pathog* 2016;12:e1005855.

568 Lauer A, Simon MA, Banning JL *et al.* Common cutaneous bacteria from the eastern red-backed
569 salamander can inhibit pathogenic fungi. *Copeia* 2007;2007:630–40.

570 Lauer A, Simon MA, Banning JL *et al.* Diversity of cutaneous bacteria with antifungal activity
571 isolated from female four-toed salamanders. *ISME J* 2008;2:145–57.

572 Leis ML, Costa MO. Initial description of the core ocular surface microbiome in dogs: Bacterial
573 community diversity and composition in a defined canine population. *Vet Ophthalmol*
574 2019;22:337–44.

575 Leis ML, Madruga GM, Costa MO. The porcine corneal surface bacterial microbiome: A
576 distinctive niche within the ocular surface. *PLoS ONE* 2021;16:e0247392–e0247392.

577 Leon AE, Hawley DM. Host responses to pathogen priming in a natural songbird host. *Ecohealth*
578 2017;14:793–804.

579 Loudon AH, Kurtz A, Esposito E *et al.* Columbia spotted frogs (*Rana luteiventris*) have
580 characteristic skin microbiota that may be shaped by cutaneous skin peptides and the
581 environment. *FEMS Microbiol Ecol* 2020;96:fiaa168.

582 McDermott AJ, Huffnagle GB. The microbiome and regulation of mucosal immunity.
583 *Immunology* 2014;142:24–31.

584 McLaren MR, Callahan BJ. Pathogen resistance may be the principal evolutionary advantage
585 provided by the microbiome. *Philos T R Soc B* 2020;375:20190592.

586 Mustafa K kh, Maulud SQ, Hamad PA. Detection of *Sphingomonas paucimobilis* and
587 antibacterial activity of *Prosopis farcta* extracts on it. *Karbala Int J Mod Sci* 2018;4:100–
588 6.

589 Nava-González B, Suazo-Ortuño I, López PB *et al.* Inhibition of *Batrachochytrium*
590 *dendrobatidis* infection by skin bacterial communities in wild amphibian populations.
591 *Microb Ecol* 2021:1–11.

592 O’Hanlon DE, Moench TR, Cone RA. Vaginal pH and microbicidal lactic acid when lactobacilli
593 dominate the microbiota. *PLoS ONE* 2013;8:e80074.

594 Oksanen J, Blanchet FG, Friendly M *et al.* vegan: Community Ecology Package. R package
595 version 2.5–2. 2018.

596 Oliver KM, Smith AH, Russell JA. Defensive symbiosis in the real world—advancing ecological
597 studies of heritable, protective bacteria in aphids and beyond. *Funct Ecol* 2014;28:341–
598 55.

599 Ozkan J, Coroneo M, Willcox M *et al.* Identification and visualization of a distinct microbiome
600 in ocular surface conjunctival tissue. *Invest Ophth Vis Sci* 2018;59:4268–76.

601 Ozkan J, Nielsen S, Diez-Vives C *et al.* Temporal stability and composition of the ocular surface
602 microbiome. *Sci Rep* 2017;7:1–11.

603 Panek M, Čipčić Paljetak H, Barešić A *et al.* Methodology challenges in studying human gut
604 microbiota – effects of collection, storage, DNA extraction and next generation
605 sequencing technologies. *Sci Rep* 2018;8:5143.

606 R Development Core Team. R: a language and environment for statistical computing. *GBIFORG*
607 2015.

608 Regoes RR. The role of exposure history on HIV acquisition: Insights from repeated low-dose
609 challenge studies. *PLoS Comput Biol* 2012;8:e1002767.

610 Regoes RR, Ebert D, Bonhoeffer S. Dose–dependent infection rates of parasites produce the
611 Allee effect in epidemiology. *Proc Royal Soc B: Biological Sci* 2002;269:271–9.

612 Reller LB, Karney WW, Beaty HN *et al.* Evaluation of cefazolin, a new cephalosporin antibiotic.
613 *Antimicrob Agents Ch* 1973;3:488–97.

614 Røssland E, Langsrud T, Granum PE *et al.* Production of antimicrobial metabolites by strains of
615 *Lactobacillus* or *Lactococcus* co-cultured with *Bacillus cereus* in milk. *Int J Food
616 Microbiol* 2005;98:193–200.

617 RStudio Team. *RStudio: Integrated Development Environment for R*. RStudio, PBC., Boston,
618 MA, USA., 2020.

619 Sassone-Corsi M, Raffatellu M. No vacancy: How beneficial microbes cooperate with immunity
620 to provide colonization resistance to pathogens. *J Immunol* 2015;194:4081–7.

621 Sekirov I, Tam NM, Jogova M *et al.* Antibiotic-induced perturbations of the intestinal microbiota
622 alter host susceptibility to enteric infection. *Infect Immun* 2008;76:4726–36.

623 Shukla SD, Budden KF, Neal R *et al.* Microbiome effects on immunity, health and disease in the
624 lung. *Clin Transl Immunol* 2017;6:e133.

625 Spekreijse D, Bouma A, Stegeman JA *et al.* The effect of inoculation dose of a highly
626 pathogenic avian influenza virus strain H5N1 on the infectiousness of chickens. *Vet
627 Microbiol* 2011;147:59–66.

628 Springer A, Fichtel C, Al-Ghalith GA *et al.* Patterns of seasonality and group membership
629 characterize the gut microbiota in a longitudinal study of wild Verreaux’s sifakas
630 (*Propithecus verreauxi*). *Ecol Evol* 2017;7:5732–45.

631 Sydenstricker KV, Dhondt AA, Ley DH *et al.* Re-exposure of captive house finches that
632 recovered from *Mycoplasma gallisepticum* infection. *J Wildlife Dis* 2005;41:326–33.

633 Thaiss CA, Zmora N, Levy M *et al.* The microbiome and innate immunity. *Nature* 2016;535:65–
634 74.

635 Thomason CA, Leon A, Kirkpatrick LT *et al.* Eye of the Finch: characterization of the ocular
636 microbiome of house finches in relation to mycoplasmal conjunctivitis. *Environ*
637 *Microbiol* 2017a;19:1439–49.

638 Thomason CA, Mullen N, Belden LK *et al.* Resident microbiome disruption with antibiotics
639 enhances virulence of a colonizing pathogen. *Sci Rep* 2017b;7:1–8.

640 Timms R, Colegrave N, Chan BHK *et al.* The effect of parasite dose on disease severity in the
641 rodent malaria *Plasmodium chabaudi*. *Parasitology* 2001;123:1–11.

642 Tung J, Barreiro LB, Burns MB *et al.* Social networks predict gut microbiome composition in
643 wild baboons. *eLife* 2015;4:e05224.

644 Vásquez A, Forsgren E, Fries I *et al.* Symbionts as major modulators of insect health: lactic acid
645 bacteria and honeybees. *PLoS ONE* 2012;7:e33188.

646 Walke JB, Becker MH, Loftus SC *et al.* Community structure and function of amphibian skin
647 microbes: an experiment with bullfrogs exposed to a chytrid fungus. *PLoS ONE*
648 2015;10:e0139848.

649 Walke JB, Belden LK. Harnessing the microbiome to prevent fungal infections: lessons from
650 amphibians. *PLoS Pathog* 2016;12:e1005796.

651 Wei Z, Yang T, Friman V-P *et al.* Trophic network architecture of root-associated bacterial
652 communities determines pathogen invasion and plant health. *Nat Commun* 2015;6:8413.

653 Weitzman CL, Sandmeier FC, Tracy CR. Host species, pathogens and disease associated with
654 divergent nasal microbial communities in tortoises. *R Soc open sci* 2018;5:181068.

655 Weyrich LS, Feaga HA, Park J *et al.* Resident microbiota affect *Bordetella pertussis* infectious
656 dose and host specificity. *J Infect Dis* 2014;209:913–21.

657 Zhu L, Clayton JB, Van Haute MJS *et al.* Sex bias in gut microbiome transmission in newly
658 paired marmosets (*Callithrix jacchus*). *mSystems* 2020;5:e00910-19.

1 **Tables**

2 **Table 1.** Sample sizes for house finches in each of ten treatment groups in a fully factorial design
3 among five *Mycoplasma gallisepticum* (MG) doses and two ocular microbiome treatments (n =
4 107 total).

5

Microbiome treatment	Pathogen Dose Concentrations (color-changing units/mL)				
	0 (MG control)	3×10^1	3×10^2	3×10^3	3×10^4
Catch-only (microbiome control)	11	8	11	12	12
Antibiotics	11	8	11	12	11

6

7

8

9

10

11

12

13

14

15

16

17

18

19

20

21 **Table 2.** Final models of pathology, pathogen load, probability of infection, and sialidase
 22 activity for experimental house finches that either had microbiomes left intact or perturbed with
 23 antibiotics prior to inoculation with *Mycoplasma gallisepticum* (MG; n = 85 inoculated birds).
 24 Bold denotes significant p-values (< 0.05). PID = post-inoculation day. Italicized p-values
 25 indicate where trends were greatly influenced by an outlier. Outlier in pathology data was a bird
 26 with severe pathology in the microbiome control, 3x10³ CCU/mL MG dose group.

27

Response	Predictors	Estimate \pm SEM	ChiSq	P	P no outlier
Pathology					
	MG dose	1.311 \pm 0.179	53.43	<0.0001	<0.0001
	Microbiome treatment	<i>−0.523 \pm 0.272</i>	3.69	<i>0.055</i>	<i>0.11</i>
	PID ²	<i>−0.002 \pm 0.0004</i>	29.05	<0.0001	<0.0001
Pathogen Load					
	MG dose x PID	<i>−0.605 \pm 0.136</i>	19.93	<0.0001	
	MG dose	1.962 \pm 0.130	227.53	<0.0001	
	Microbiome treatment	<i>−0.360 \pm 0.278</i>	1.68	0.19	
	PID	0.975 \pm 0.446	4.78	0.029	
Probability of Infection					
	MG dose	2.993 \pm 0.629	91.17	<0.0001	
	Microbiome treatment	<i>−0.652 \pm 0.596</i>	1.29	0.26	
MG Sialidase Phenotype					
(n = 48)	MG dose	<i>−13.48 \pm 12.32</i>	0.014	0.91	
	Microbiome treatment	<i>−5.62 \pm 17.83</i>	0.048	0.83	
	Temporal group	<i>−41.59 \pm 17.47</i>	8.30	0.006	

28

29

30

31

32

33

34 **Figure Legends**

35 **Figure 1.** Experimental timeline based on post-inoculation day (PID) with respect to inoculation
36 with *Mycoplasma gallisepticum* (MG). To detect whether the protective effects of an intact
37 ocular microbiome vary with the inoculation dose of MG in house finches, we collected: P =
38 pathology scores and nucleic acid swab samples, C = conjunctival culture swab samples from a
39 subset of birds to confirm antibiotic efficacy (Supplemental Materials), M = MG sialidase
40 phenotype swabs, and B = blood samples to determine antibody levels (Supplemental Materials).

41

42 **Figure 2.** Intact ocular microbiomes were not protective against *Mycoplasma gallisepticum*
43 (MG) disease or infection severity in house finches. (a) Pathology scores for the two highest MG
44 dose concentrations (only two doses shown for ease of visualization, but see Figure S2 for lower
45 dose results) across post-inoculation days (PID). Squares indicate 3×10^3 CCU/mL MG dose.
46 Triangles indicate 3×10^4 CCU/mL MG dose. (b) MG load on days 3 and 13 post-inoculation
47 were predicted by MG dose, PID, and their interaction, but not antibiotic treatment. Only birds in
48 the four treatment groups with MG dose > 0 are shown for visual clarity. In both panels, open
49 symbols signify birds given antibiotic to perturb the resident microbiome, and closed symbols
50 signify control birds not given antibiotic. Points and bars signify mean and standard error.

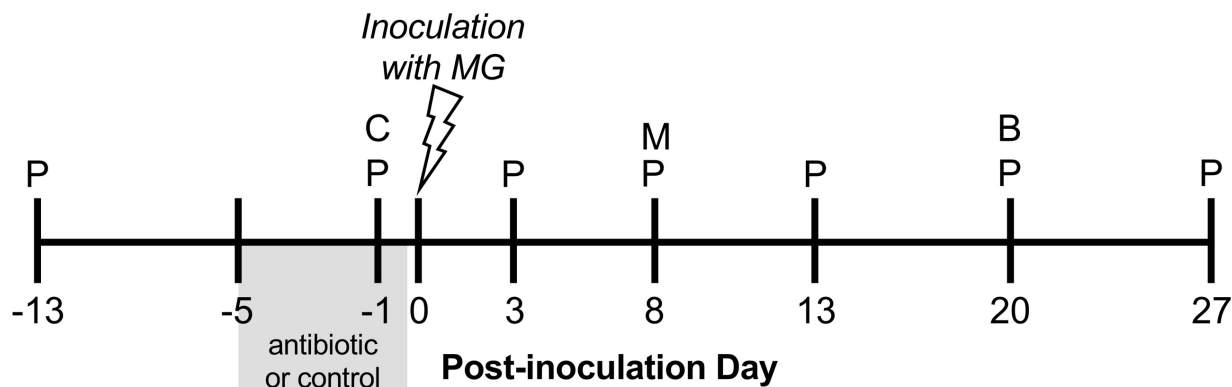
51

52 **Figure 3.** Abundant genera in the resident ocular microbiomes sampled in 2019 (this
53 experiment) compared with those sampled in 2016 (far right; Thomason et al. 2017b). All
54 microbiomes were sampled either 13 days or 1 day prior to inoculation with *M. gallisepticum*
55 and thus represent resident microbiome communities (birds given ocular antibiotics were
56 excluded for clarity). Proportions based on relative abundance of rarefied reads. Samples

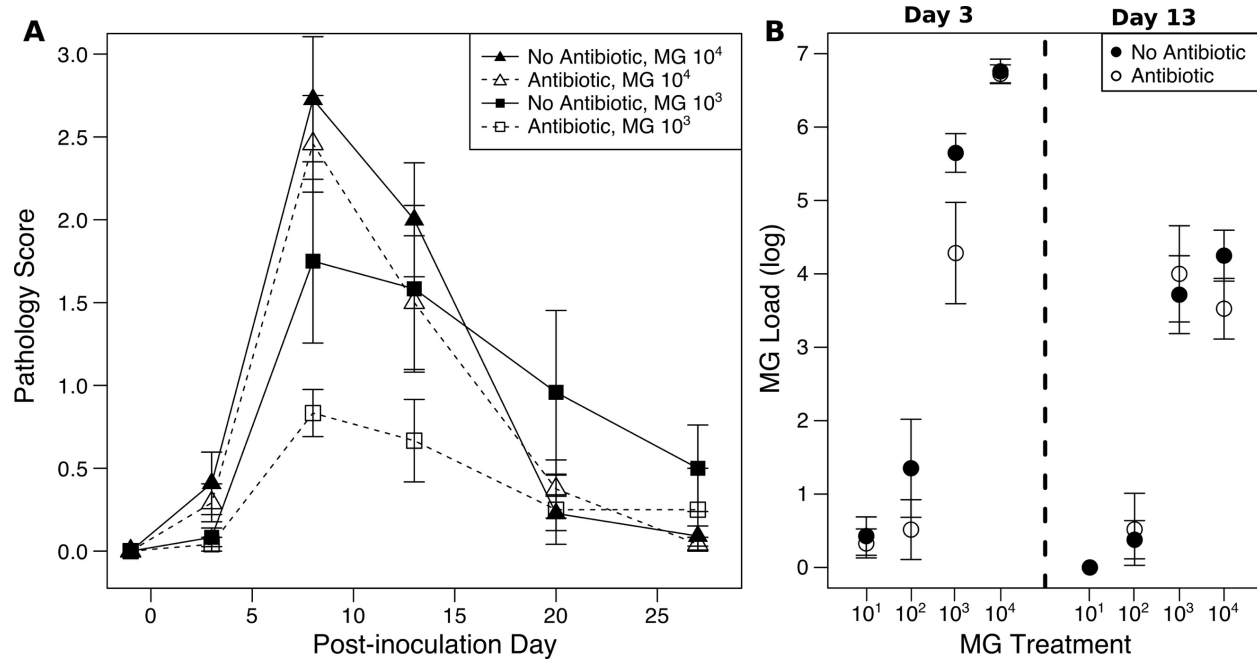
57 grouped by post-inoculation day and treatment. Included genera account for at least 2% of the
58 reads in each sample type.

59

60 Figure 1



63 Figure 2

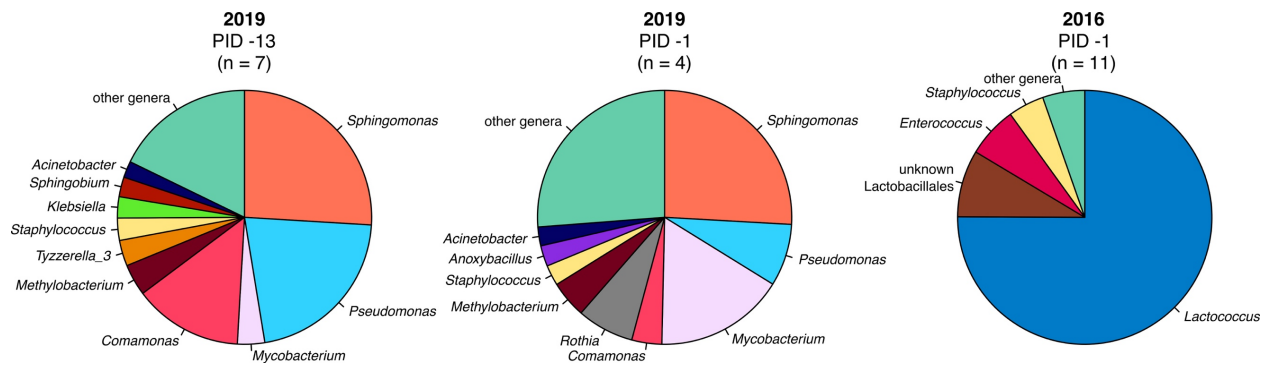


64

65

66

67 Figure 3



68